ARTICLE

Check for updates

Journal of
Sensor Science and Technology

The Korean Sensors Society

Bilateral Ground Reaction Force Decomposition Using an IMU-Based Neural Network in Gait and Non-Gait Movements

Ji Hoon Park[1] and Jung Keun Lee[1,+]

[1] *School of ICT, Robotics and Mechanical Engineering, Hankyong National University, 327 Jungang–ro, Anseong, Gyeonggi 456-749, Republic of Korea*

Cite This: *J. Sens. Sci. Technol. Vol. 35, No. 3 (2026) 225-232*

https://doi.org/10.46670/JSST.2026.35.3.225

ABSTRACT: Bilateral ground reaction force (GRF) is an important variable in gait analysis and sports biomechanics. However, measuring bilateral GRF requires a split-belt instrumented treadmill or multiple force plates, and cost and space constraints limit its availability. In such cases, only the total GRF may be available from a single force plate or single-belt system, requiring decomposition into bilateral GRF. Previous studies have focused mainly on gait and remain limited for non-gait movements. Accordingly, this study proposes an inertial measurement unit-based neural network (NN) to decompose total GRF into bilateral GRF for gait and non-gait movements. The performance was compared across segment configurations and against the smooth transition assumption (STA) method. In gait, the difference in the root mean squared error (RMSE) among the NN methods was within 0.03 N/kg, and all NN methods showed lower RMSEs in walking (0.38–0.42 N/kg) than STA (0.84 N/kg). For non-gait movements, the thighs-shanks-feet configuration showed the best performance, and the shanks configuration showed similar performance, with an RMSE difference within 0.05 N/kg, whereas the feet and right shank configurations showed inferior performance. The results support the shanks configuration as a practical option and demonstrate the applicability of the proposed method to gait and non-gait movements.

KEYWORDS: *Bilateral ground reaction force, Decomposition, Inertial measurement unit, Neural network, Gait, Non-gait movements*

1. INTRODUCTION

The bilateral ground reaction force (GRF) is a representative external force acting during human movement and is an important kinetic variable for the analysis of inverse dynamics-based joint reaction forces and lower-limb joint moments [1-3]. It is also widely used in gait analysis, rehabilitation assessment, and sports biomechanics [4-7]. Directly measuring the bilateral GRF requires equipment such as force plates or a split-belt instrumented treadmill, but its use is limited by cost and space requirements [8,9]. Consequently, in certain settings, only the total GRF is available from a single force plate or a single-belt instrumented treadmill, and under such conditions, a method is required to decompose the total 3-axis GRF into bilateral 3-axis GRFs [10,11].

Existing bilateral GRF decomposition methods have focused primarily on gait. Representative methods include those based on the center of pressure trajectory [12,13] and the smooth transition assumption (STA) [14,15]. However, these methods commonly depend on gait events or the temporal structure of the double-support phase.

Regarding non-gait movements, a method has been reported to estimate the independent vertical GRF of each foot during a standing test using a single force plate [16]. However, such studies have focused primarily on the vertical component under standing conditions, and studies addressing bilateral 3-axis GRF decomposition during dynamic non-gait movements remain limited. Moreover, to the best of the authors' knowledge, no method has yet been reported to decompose the total 3-axis GRF into bilateral 3-axis GRFs for both gait and non-gait movements.

Inertial measurement units (IMUs) are well-suited for measuring kinematic information from body segments, as

[+]Corresponding author: jklee@hknu.ac.kr
Received : Apr. 8, 2026, Revised : Apr. 15, 2026, Accepted : Apr. 24, 2026

they are subject to minimal spatial constraints and can be used in various environments [9,17]. Previous studies have reported that kinetic waveforms, including the GRF, can be estimated using IMUs not only for gait but also for various other movements [18,19]. This suggests that IMUs contain key kinematic information capable of explaining the kinetic characteristics of human movement. Therefore, IMUs may provide meaningful kinematic information for the decomposition of total GRF into bilateral GRF in both gait and non-gait movements.

For the practical wearable application of this IMU-based approach, both decomposition accuracy and practicality should be considered. Recent wearable sensor-based studies have suggested that practical configurations that minimize the number of sensors are an important design direction for improving practicality [8,20]. In bilateral GRF decomposition as well, maintaining acceptable performance while reducing the sensor burden requires that even limited segment configurations provide sufficient key kinematic information for decomposition when one IMU is attached to each segment. However, as the number of sensors decreases, the available information becomes more limited, and an approach is needed to effectively model the complex relationship between the input information and bilateral GRF under such conditions. In this respect, neural networks (NNs) offer a useful approach [21]. NNs can acquire complex nonlinear relationships between input and output variables to effectively model patterns inherent in the data [22,23]. Thus, by learning the complex relationships between IMU-based kinematic features and bilateral GRF, an NN model may provide effective decomposition performance even with limited segment configurations.

Accordingly, this study proposes a 6-axis-IMU-based NN model to decompose total GRF into bilateral GRF for both gait and non-gait movements. In addition, GRF decomposition performance and practicality are analyzed across different body segment configurations to propose a suitable practical configuration.

2. METHOD

2.1 GRF Decomposition Method

In this study, an IMU-based NN model was developed to decompose the total GRF into bilateral GRFs. The NN input consisted of time-series data and constant inputs. The time-series data included the 3-axis total GRF and, for the selected body segments, the 3-axis angular velocity, 3-axis acceleration of the segment center of mass, and 3-axis attitude vector estimated from the IMU signals. The constant inputs were body mass and body height. In this study, to evaluate the effect of segment configuration on decomposition performance, the NNs were developed using a consistent network structure and training procedure across multiple segment configurations. Accordingly, the body segments used as inputs varied depending on the segment configuration. The NN output was the 3-axis decomposition variable $\mathbf{d}=\begin{bmatrix} d_x & d_y & d_z \end{bmatrix}^T$. The variable $\mathbf{d}$ was designed to account for the different decomposition characteristics of the horizontal and vertical components of the total GRF. For the horizontal components, because the GRFs of the two feet may act in opposite directions, d_x and d_y were designed as deviation terms representing the difference in force between the two feet. For the vertical component, because the GRFs of the two feet act in the same direction, d_z was designed as a ratio term representing the load-sharing between the left and right feet. In addition, to prevent unrealistic vertical GRF decomposition, d_z was constrained to a range between 0 and 1. Using this $\mathbf{d}$, the total GRF can be decomposed such that the sum of the bilateral GRFs matches the total GRF. The decomposed right GRF, $\hat{\mathbf{F}}_R$, was calculated from $\mathbf{d}$ estimated by the NN and the total GRF, $\mathbf{F}_T$, as follows.

$$\hat{F}_{R,x} = d_x + \frac{F_{T,x}}{2} \tag{1}$$

$$\hat{F}_{R,\mathrm{y}} = d_y + \frac{F_{T,\mathrm{y}}}{2} \tag{2}$$

$$\hat{F}_{\mathrm{R,z}} = d_z F_{T,z} \tag{3}$$

Using the calculated $\hat{\mathbf{F}}_R$, the decomposed left GRF, $\hat{\mathbf{F}}_L$, was obtained as follows.

$$\hat{\mathbf{F}}_{\mathrm{L}} = \mathbf{F}_T - \hat{\mathbf{F}}_R \tag{4}$$

Fig. 1 shows the framework of the bilateral GRF decomposition method.

The decomposition NN consisted of a gated recurrent unit (GRU) and a multilayer perceptron (MLP). After standardization using the mean and standard deviation, the time-series input data were fed into two stacked GRU layers, each with 256 hidden units. The hidden state output from the GRU was then fed into the MLP together with the constant inputs. The MLP consisted of two hidden fully connected layers, each with 256 hidden units, and an output layer. The ReLU was used as the activation function for the hidden layers. In addition, dropout rates of 0.1 and 0.5 were applied to the hidden layers of the GRU and MLP, respectively. To mitigate training imbalance caused by differences in magnitude among the output components, min-max normalization was applied to the outputs, and the values were restored to their original range through inverse transformation.

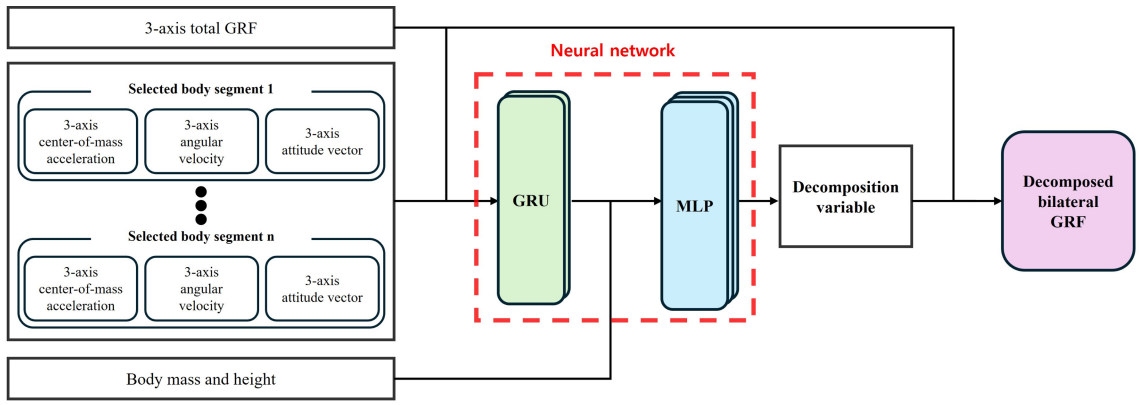

Fig. 1. Framework of the bilateral GRF decomposition method.

Table 1. Subject information.

Subject No.	Gender	Age (year)	Weight (kg)	Height (m)
1	Male	26	95.43	1.65
2	Male	30	83.89	1.73
3	Male	23	98.06	1.78
4	Male	25	103.73	1.73
5	Male	26	81.20	1.80
6	Male	24	70.10	1.73
7	Male	26	81.30	1.71
8	Male	25	64.09	1.76
9	Female	22	69.54	1.63
10	Male	28	76.56	1.80
11	Female	24	62.09	1.60
12	Male	23	63.17	1.68

Mean squared error was used as the loss function, the Ranger optimizer was used for optimization, and gradient clipping was applied to improve training stability. For NN training, the learning rate, batch size, input sequence length, number of epochs, and gradient clipping threshold were set to 0.001, 64, 300, 100, and 1, respectively.

2.2 Experimental Validation

This study was conducted using a dataset that was previously collected in the authors' laboratory, and this dataset is publicly available [24]. The experimental setup consisted of IMUs, a front-to-rear split-belt instrumented treadmill, and an optical motion capture (OMC) system. One IMU was attached to each thigh, shank, and foot on both sides. The instrumented treadmill independently measured bilateral GRF using force plates embedded in each belt, and in the non-gait trials, the left and right feet were positioned on separate belts so that the GRF of each foot could be measured individually. The OMC system was used to obtain the positions of markers attached to the IMU clusters and segments, and these data were leveraged to determine the orientations of the IMUs and segments. The obtained IMU-to-segment orientation information was then used to estimate the kinematic variables of each segment from the IMU signals. The IMU-to-segment orientation may also be acquired using a measurement system other than the OMC system. Uncertainties in the resulting kinematic variables may affect the decomposition performance. All measurement devices were temporally synchronized using a hardware trigger and post-processing alignment.

Twelve subjects participated in the experiment, and each subject performed 12 gait trials and 10 non-gait movement trials. Table 1 presents the subject information. The gait trials consisted of nine walking trials and three running trials on the instrumented treadmill, and the non-gait trials consisted of two trials for each of weight shift, half squat, full squat, side squat, and squat jump. Weight shift involved shifting body weight laterally while alternately lifting one leg. Half squat and full squat involved repeated flexion of the knees and hips while moving the center of mass vertically with both feet in contact with the ground, and the full squat was performed at a greater squat depth than the half squat. Side squat involved shifting the center of mass laterally with both feet in contact with the ground, while the squat jump comprised a preparatory squat followed by a jump and landing. Walking trials were performed for 2 min, running trials for 90 s, and non-gait trials for 1 min each. For the training and validation of the NN, continuous intervals spanning 50 gait cycles were used for the gait trials, and 40-s intervals were used for the non-gait trials.

The performance of the decomposition NN was evaluated using group-based 4-fold cross-validation. The 12 subjects were randomly divided into four groups, and in each fold, one group was used as the validation set and the remaining groups were used as the training set. Thus, the validation in each fold

Table 2. Method-wise RMSE for gait and non-gait movements, calculated from the right GRF error magnitude (N/kg). Values in parentheses indicate standard deviations.

Movements		M1 (thighs-shanks-feet)	M2 (shanks)	M3 (feet)	M4 (right shank)	M5 (STA)
Gait	Walking	0.38 (0.15)	0.38 (0.21)	0.38 (0.11)	0.42 (0.33)	0.84 (0.14)
	Running	0.30 (0.08)	0.28 (0.07)	0.28 (0.08)	0.30 (0.11)	–
	Average	0.34 (0.11)	0.33 (0.14)	0.33 (0.09)	0.36 (0.22)	–
Non-gait	Weight shift	0.35 (0.11)	0.37 (0.17)	0.50 (0.27)	0.59 (0.11)	–
	Half squat	0.28 (0.09)	0.35 (0.14)	0.56 (0.50)	0.46 (0.60)	–
	Full squat	0.29 (0.08)	0.36 (0.14)	0.58 (0.46)	0.45 (0.22)	–
	Side squat	0.38 (0.09)	0.43 (0.14)	1.19 (0.38)	0.56 (0.17)	–
	Squat jump	0.46 (0.08)	0.50 (0.10)	0.81 (0.45)	0.65 (0.18)	–
	Average	0.35 (0.09)	0.40 (0.14)	0.73 (0.41)	0.54 (0.27)	–

was performed on three subjects who had not been utilized for training. In addition, to examine performance differences across segment configurations, four configurations were defined using the thigh, shank, and foot segments, and their performances were compared. Method 1 (M1) used the thighs-shanks-feet configuration, Method 2 (M2) used the shanks configuration, Method 3 (M3) used the feet configuration, and Method 4 (M4) used the right shank configuration. For a comparison with the existing gait decomposition method, the STA method proposed by Ren et al. [14] was reproduced and included as Method 5 (M5). The STA assumes that the GRF of the trailing foot decreases smoothly as toe-off approaches during the double support (DS), first estimates the trailing-foot GRF, and then calculates the leading-foot GRF by subtracting the estimated trailing-foot GRF from the total GRF. Because the STA was developed for walking, it was applied only to the walking trials and not to running, which includes a flight phase without a double-support period. The ground-truth (GT) gait events were used to eliminate the effect of gait-event uncertainty. In contrast, because the NN did not directly use gait-event information

as an input, its decomposition performance was evaluated for left single support (LSS), right single support (RSS), and the DS to examine how the performance varied across gait phases. Performance was evaluated using the root mean squared error (RMSE) calculated from the error magnitude.

3. RESULTS AND DISCUSSIONS

3.1 Results

Both the proposed NN and the STA are methods for decomposing the total GRF into bilateral GRFs such that the sum of the decomposed bilateral GRFs matches the total GRF. Therefore, the errors in the decomposed left and right GRFs are equal in magnitude and opposite in direction. Accordingly, the decomposition performance of each method was evaluated based on the decomposed right GRF.

In addition, all results were normalized by each subject's body mass and are reported in N/kg.

Table 2 shows the RMSE for each method, calculated from the error magnitude of the decomposed right GRF. M1 showed average RMSEs of 0.34 and 0.35 N/kg for gait and non-gait, respectively, indicating similar performance across the two movement categories. It also showed the lowest average RMSE in non-gait and the best overall performance. M2 showed average RMSEs of 0.33 and 0.40 N/kg for gait and non-gait, respectively; although the RMSE increased slightly in non-gait relative to gait, its overall performance remained reasonably good. For M3, the non-gait RMSE was 0.40 N/kg higher than the gait RMSE, and its non-gait RMSE was the largest among all methods. M3 showed the poorest performance in most non-gait movements, especially in the side squat, where the RMSE reached 1.19 N/kg. For M4, the non-gait RMSE was 0.18 N/kg higher than the gait RMSE. For walking, the RMSE of M5 was 0.84 N/kg, which was twice that of M4, the second poorest-performing method. For gait, the difference in the average RMSE among the NN-based methods was within 0.03 N/kg. For non-gait movements, the difference in the average RMSE between M1 and M2 was small at 0.05 N/kg, whereas the corresponding differences for M3 and M4 relative to M1 were 0.38 and 0.19 N/kg, respectively.

Fig. 2 shows the decomposed right GRF and error magnitude for each method over a selected interval of walking, with the bottom plot showing the error magnitude with M5 omitted. The NN methods generally showed similar error magnitudes, whereas the error magnitude of M5 increased up

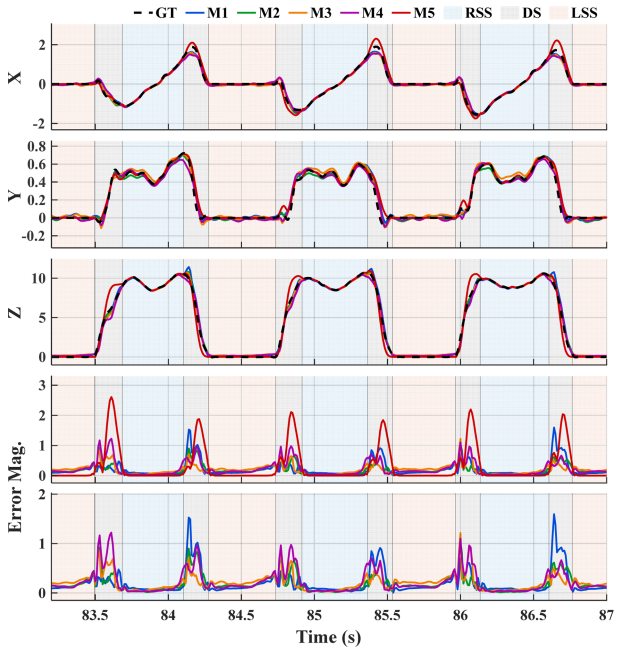

Fig. 2. Zoomed-in view of the decomposed right GRF (N/kg) and error magnitude during walking, with the bottom panel showing the error magnitude excluding M5.

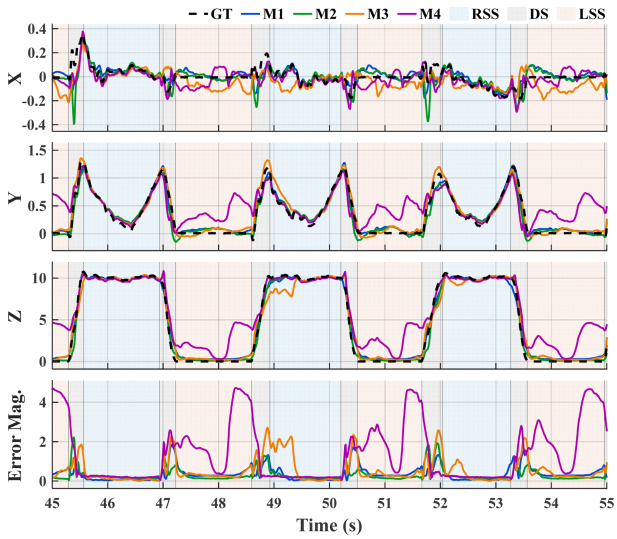

Fig. 3. Zoomed-in view of the decomposed right GRF (N/kg) and error magnitude during weight shift.

to approximately 2.5 N/kg and was overall larger than those of the NN-based methods. Figs. 3 and 4 show the decomposed right GRF and error magnitude for each method over selected intervals of weight shift and the side squat, respectively. In Fig. 3, the results of M1 and M2 were similar to the GT, whereas those of M3 and M4 exhibited trends that differed slightly from the GT. The error magnitude of M3 was large in some intervals, whereas that of M4 was low during RSS but high in DS and LSS. In Fig. 4, the results of M1, M2, and M4 closely

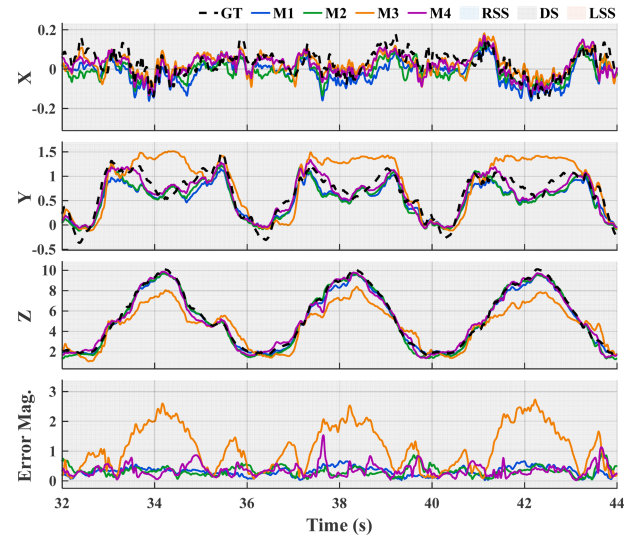

Fig. 4. Zoomed-in view of the decomposed right GRF (N/kg) and error magnitude during the side squat.

matched the GT across all axes, whereas M3 showed clear differences from the GT on the y- and z-axes. The error magnitudes of M1 and M2 were reasonably low. For M3, the error magnitude exceeded approximately 2 N/kg in the interval where the GT increased on the z-axis, representing the largest error magnitude among all methods. M4 tended to show relatively large errors in some intervals. Fig. 5 shows the subject-wise average RMSEs of M1 and M2. Across the subjects, the RMSE difference between M1 and M2 ranged from 0.01 to 0.11 N/kg, indicating that the performance of M1 and M2 was similar for most subjects.

3.2 Discussions

Gait is characterized by a cyclic pattern and by a relatively regular transfer of body weight from one foot to the other during the DS phase. Accordingly, the load-sharing pattern between the two feet follows a relatively regular pattern, which may have provided favorable conditions for bilateral GRF decomposition. Indeed, all NN methods tended to outperform the STA during walking. In addition, the performance differences among the segment configurations selected in this study were small in gait. This suggests that even limited segment configurations can provide sufficient information for the decomposition. Furthermore, although gait-event information was not provided as input, the errors were relatively small in LSS and RSS. This may be attributed to the fact that the NNs learned periodic patterns related to the gait cycle and gait events from the continuous kinematic information captured by the IMUs. The decomposition NN also showed a lower RMSE during running than during

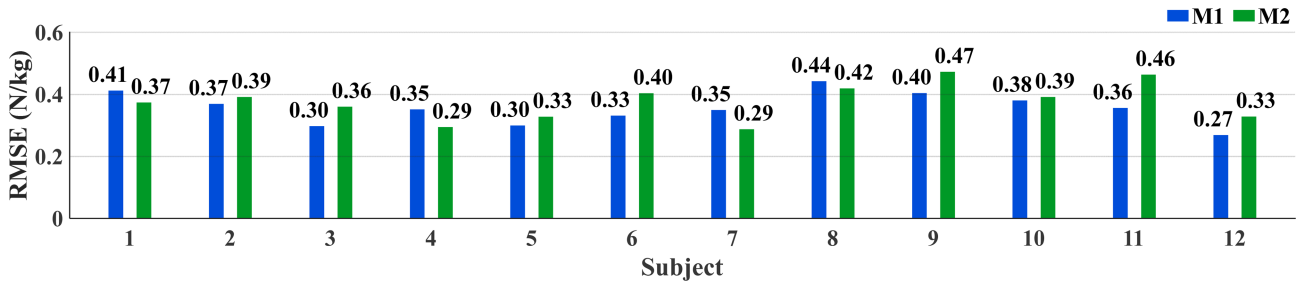

Fig. 5. Subject-wise RMSEs for M1 and M2, calculated from the right GRF error magnitude (N/kg).

walking. This is likely because the DS interval, in which relatively large errors tend to occur, is shorter in running than in walking.

M2, M3, and M4 tended to show higher RMSEs during non-gait movements than during gait. This may be attributed to the fact that, unlike gait, non-gait movements do not exhibit clear regularity and, in many cases, involve postural changes in the lower-limb segments together with changes in bilateral GRF while both feet remain in contact with the ground, which may make decomposition relatively difficult. Therefore, in non-gait movements, the segment configuration becomes increasingly important because it determines whether sufficient kinematic information for the decomposition process can be obtained.

M1, which used information from the greatest number of segments, showed the best overall performance across both gait and non-gait movements. This indicates that the simultaneous use of the kinematic information obtained from the bilateral thighs, shanks, and feet was advantageous for bilateral GRF decomposition. The squat jump is a dynamic non-gait movement consisting of a preparatory squat, jump, and landing, and the decomposition NN also showed acceptable performance for this movement. Therefore, the proposed method may also be applicable to certain dynamic movements with similar characteristics, such as jump landings. However, achieving this performance requires six

IMUs, which limits the practical application because of the high sensor burden.

Despite being a simple configuration using only the shanks, M2 showed acceptable performance, with RMSEs within 0.07 N/kg of those of M1 across both gait and non-gait movements. In other words, M2 showed performance comparable to that of M1 even though it did not use information from the bilateral thighs or feet. This indicates that the bilateral shanks can provide sufficient information for the decomposition in both gait and non-gait movements. In particular, in non-gait movements such as weight shift, in which one leg is lifted, and side squat, in which the center of mass shifts, information on the orientations and relative motions of the bilateral shanks appears to be effective for the decomposition. Therefore, M2 can be regarded as the most practical configuration when both performance and practicality are considered.

M3, the configuration utilizing only the feet, exhibited acceptable performance in gait but the poorest performance in most non-gait movements. In particular, its performance decrease was most pronounced during the side squat. This can be attributed to the fact that, when both feet remain continuously in contact with the ground, changes in foot-segment posture are limited and do not directly reflect kinematic information related to the hip or knee.

M4, the simplest configuration using only the right shank, showed acceptable performance in gait. This indicates that the kinematic information from a unilateral shank alone can provide sufficient information for the decomposition. However, in non-gait movements, it showed somewhat inferior performance compared with M1 and M2. In particular, during the LSS interval of weight shift, the error of M4, which used only the information from the right shank, was larger than that of M2, which used bilateral shank information. These results show that unilateral segment information alone has limitations in providing the information required for bilateral GRF decomposition during non-gait movements. These findings suggest that bilateral information is important for decomposition in non-gait movements.

4. CONCLUSIONS

This study proposes an IMU-based NN method for decomposing total GRF into bilateral GRF during gait and non-gait movements and compares the decomposition performance and practicality among several segment configurations. Unlike previous studies, which have mainly focused on gait, this study presents a bilateral 3-axis GRF decomposition method covering both gait and non-gait movements and demonstrates its applicability across these movement types. In particular, during walking, all NN methods showed lower RMSEs than STA, thereby supporting the validity of the proposed method.

In gait, all NN methods showed similar performance. This

suggests that, when the total GRF is available, the bilateral GRF decomposition in gait can be achieved even with limited segment configurations. In other words, these findings indicate that, during gait, sufficient kinematic information for the decomposition can be obtained even from a relatively small number of segments. In contrast, during non-gait movements, performance differences across segment configurations were more pronounced than those observed in gait. In particular, the method using bilateral shanks maintained performance comparable to that of the method using the most segment information, whereas the feet and unilateral shank configurations showed degraded performance in some movements. These results indicate that, for bilateral GRF decomposition during non-gait movements, the selection of segments that can reflect movement-specific postural changes and bilateral information is important. Therefore, the bilateral shank configuration can be considered the most appropriate configuration when both performance and practicality are taken into account, as it reduces the sensor burden while maintaining stable performance across gait and non-gait movements.

The proposed method does not explicitly use gait-event information or foot-ground contact information; consequently, errors were observed in the single-support intervals even though the total GRF was available. Therefore, future studies should consider an approach in which gait events and foot-ground contact information are estimated and used as auxiliary inputs to improve bilateral GRF decomposition performance during the single-support intervals.

CRediT Authorship Contribution Statement

Ji Hoon Park: Investigation, Data curation, Methodology, Writing – Original Draft, Writing – Review & Editing. **Jung Keun Lee:** Supervision, Methodology, Conceptualization, Writing – Review & Editing.

Declaration of Competing Interest

The authors declare that they have no known competing financial interests or personal relationships that could have appeared to influence the work reported in this paper.

Acknowledgements

This research received no external funding.

REFERENCES

[1] J.E. Langenderfer, P.J. Laz, A.J. Petrella, P.J. Rullkoetter, An efficient probabilistic methodology for incorporating uncertainty in body segment parameters and anatomical landmarks in joint loadings estimated from inverse dynamics, J. Biomech. Eng. 130 (2008) 014502.

[2] R.W. Bisseling, A.L. Hof, Handling of impact forces in inverse dynamics, J. Biomech. 39 (2006) 2438–2444.

[3] R. Pàmies-Vilà, J.M. Font-Llagunes, J. Cuadrado, F.J. Alonso, Analysis of different uncertainties in the inverse dynamic analysis of human gait, Mech. Mach. Theory 58 (2012) 153–164.

[4] M.K. Seeley, B.R. Umberger, R. Shapiro, J.W. Chow, A test of the functional asymmetry hypothesis in walking, Gait Posture 28 (2008) 24–28.

[5] M.G. Bowden, C.K. Balasubramanian, R.R. Neptune, S.A. Kautz, Anterior-posterior ground reaction forces as a measure of paretic leg contribution in hemiparetic walking, Stroke 37 (2006) 872–876.

[6] G. Kuntze, W.I. Sellers, N. Mansfield, Bilateral ground reaction forces and joint moments for lateral sidestepping and crossover stepping tasks, J. Sports Sci. Med. 8 (2009) 1–8.

[7] J. Yanci, J. Camara, Bilateral and unilateral vertical ground reaction forces and leg asymmetries in soccer players, Biol. Sport 33 (2016) 179–183.

[8] Y. Zhu, D. Xia, H. Zhang, Using wearable sensors to estimate vertical ground reaction force based on a transformer, Appl. Sci. 13 (2023) 2136.

[9] A. Karatsidis, G. Bellusci, H.M. Schepers, M. de Zee, M.S. Andersen, P.H. Veltink, Estimation of ground reaction forces and moments during gait using only inertial motion capture, Sensors 17 (2016) 75.

[10] B. Samadi, M. Raison, L. Ballaz, S. Achiche, Decomposition of three-dimensional ground-reaction forces under both feet during gait, J. Musculoskelet. Neuronal Interact. 17 (2017) 283–291.

[11] G.M. Meurisse, F. Dierick, B. Schepens, G.J. Bastien, Determination of the vertical ground reaction forces acting upon individual limbs during healthy and clinical gait, Gait Posture 43 (2016) 245–250.

[12] B.L. Davis, P.R. Cavanagh, Decomposition of superimposed ground reaction forces into left and right force profiles, J. Biomech. 26 (1993) 593–597.

[13] L. Ballaz, M. Raison, C. Detrembleur, Decomposition of the vertical ground reaction forces during gait on a single force plate, J. Musculoskelet. Neuronal Interact. 13 (2013) 236–243.

[14] L. Ren, R.K. Jones, D. Howard, Whole body inverse dynamics over a complete gait cycle based only on measured kinematics, J. Biomech. 41 (2008) 2750–2759.

[15] D. Villeger, A. Costes, B. Watier, P. Moretto, An algorithm to decompose ground reaction forces and moments from a single force platform in walking gait, Med. Eng. Phys. 36 (2014) 1530–1535.

[16] A. Schmedling, E. Macho, F.J. Campa, R. Valenzuela, M. Diez, J. Corral, et al., Determining the ground reaction force value and location for each foot during bipedal stance exercises from a single forceplate, Sensors 25 (2025) 4796.

[17] A. Ancillao, S. Tedesco, J. Barton, B. O'Flynn, Indirect measurement of ground reaction forces and moments by means of wearable inertial sensors: A systematic review, Sensors 18 (2018) 2564.

[18] S.R. Donahue, M.E. Hahn, Estimation of gait events and kinetic waveforms with wearable sensors and machine learning when running in an unconstrained environment, Sci. Rep. 13 (2023) 2339.
[19] T. Koshio, N. Haraguchi, T. Takahashi, Y. Hara, K. Hase, Estimation of ground reaction forces during sports movements by sensor fusion from inertial measurement units with 3D forward dynamics model, Sensors 24 (2024) 2706.
[20] B. Yılmazgün, J. Weber, T. Stein, S. Sell, B.J. Stetter, Predicting 3D ground reaction forces across various movement tasks: A convolutional neural network study comparing different inertial measurement unit configurations, J. Biomech. 192 (2025) 112888.
[21] E. Halilaj, A. Rajagopal, M. Fiterau, J.L. Hicks, T.J. Hastie, S.L. Delp, Machine learning in human movement biomechanics: Best practices, common pitfalls, and new opportunities, J. Biomech. 81 (2018) 1–11.
[22] S.E. Oh, A. Choi, J.H. Mun, Prediction of ground reaction forces during gait based on kinematics and a neural network model, J. Biomech. 46 (2013) 2372–2380.
[23] M. Mundt, A. Koeppe, S. David, F. Bamer, W. Potthast, B. Markert, Prediction of ground reaction force and joint moments based on optical motion capture data during gait, Med. Eng. Phys. 86 (2020) 29–34.
[24] C.J. Lee, J.K. Lee, A multimodal dataset of full-body kinematics and kinetics from laboratory- and wearable-based systems, Zenodo. https://doi.org/10.5281/zenodo.17188466, 2025 (accessed 8 April 2026).